Ecosystem Water Use Efficiency Response to Drought Over Southwest China

Ali Mokhtar[1,2], Hongming He[1,3*], Karam Alsafadi[4], Safwan Mohammed[5], Wenming He[6*], Yu Li[7*], Hongfei Zhao[1], Nazir Muhammad Abdullahi[8], Yeboah Gyasi-Agyei[9]

[1]State of Key Laboratory of Soil Erosion and Dryland Farming on Loess Plateau, Northwest Agriculture and Forestry University; Institute of Soil and Water Conservation, Chinese Academy of Sciences and Ministry of Water Resources, Yangling 712100, China;
[2]Department of Agricultural Engineering, Faculty of Agriculture, Cairo University, Giza 12613, Egypt.
[3]School of Geographic Sciences, East China Normal University, Shanghai 210062, China.
[4]School of Geographical Sciences, Nanjing University of Information Science and Technology, Nanjing 210044, China.
[5]University of Debrecen, Debrecen 4032, Hungary
[6]Guangdong Provincial Key Laboratory of Conservation and Precision Utilization of Characteristic Agricultural Resources in Mountainous Areas, School of Chemistry and Environment, Jiaying University, Meizhou, Guangdong, 514015, China
[7]Institute of Geographic Sciences and Natural Resources, Chinese Academy of Sciences, Beijing 101400, China
[8]College of Economics and Management, Northwest A&F University, Yangling 712100, China
[9]School of Engineering and Built Environment, Griffith University, Nathan QLD 4111, Australia
*Corresponding author: Hongming He, hongming.he@yahoo.com; Tel.: (+86-29-87012884; 712100).
*Corresponding author: Wenming He, hwmjim@163.com
*Corresponding author: Yu Li, liyuljy@163.com

Ecosystem Water Use Efficiency Response to Drought Over Southwest China

Abstract: Drought is showing an increasing trend as a result of the significant variation in precipitation and temperature in China. This study investigated the impacts of drought on ecosystem water use efficiency (WUE) in southwest China. The spatiotemporal distribution of drought and ecosystem WUE were analyzed through integrated approaches based on observed climate and satellite remote sensing datasets to understand the response of ecosystem WUE to drought. Also, the impacts of climatic variables on gross primary productivity (GPP), evapotranspiration (ET) and WUE have been discussed. More than 30% of the total area can be categorized as suffering moderate drought. Six drought events (autumn 2006, autumn 2009, winter 2010, summer 2011, autumn 2011 and winter 2013) were identified during the period of 2001-2016. The average monthly WUE was 2.37 gC/kgH_2O, showing a decreasing trend under the combined effects of drought and other environmental factors. Autumn 2006 exhibited the highest significant positive effect of drought on WUE on more than 80% of the total area that concentrated in the forest, shrubland, savanna and agriculture ecosystems. The results of this study have implications for ecosystem management and climate policy making that could allow implementing feasible water use strategies under a warming climate.

Keywords: Drought; Water use efficiency; Gross primary productivity; Spatiotemporal variability; MODIS datasets.

1. Introduction

Drought is an intermittent disturbance when water supply does not meet the demand for a long time (Zhao and Running, 2010), and can bring profound effects on carbon-water fluxes in terrestrial ecosystems at the global and regional scales (Sheffield et al., 2012, Yu et al., 2014). Extreme droughts happened every two years during the period of 1990–2007 in China which resulted in annual grain loss of around 39.2 million tons that decreased the gross domestic product by 1.47% (Zhai et al., 2010). Globally, increasing evaporation due to increasing temperature lead to drought without any changes in precipitation. Moreover, the frequency and intensity of drought are also increasing dramatically due to global warming (Zhang et al., 2018, Sheffield and Wood, 2008, Trenberth et al., 2013, Mokhtar et al., 2021). In recent years, southwest China has suffered serious droughts that caused disastrous effects on the socioeconomic, ecosystems and agricultural sector, especially in 2006 when it caused crop failure on 0.3 million hectares of agricultural areas and water scarcity to more than 18 million people (Yang et al., 2012, Zhang et al., 2012, Wang et al., 2015a). The frequency of occurrence of dry and wet years in southern China were lower than northwest China during the period of 1961-2005 (Zhai et al., 2010).

The ecosystem in China is huge and diverse, including a broad range of tropical and temperate climate, and boreal forest, agriculture, grass, savanna and urban land cover. It plays a vital role in the global and regional carbon cycle, and is slowly increasing the concentration of atmospheric CO_2 (Mu et al., 2015, Quere et al., 2012). Due to the close relationship between ecosystem dynamics and available water, drought can be restrictive to ecosystem growth and the distribution pattern and types (Narasimhan and Srinivasan, 2005, Vicenteserrano et al., 2012, Vicente-Serrano, 2015). Several previous studies have indicated that ecological programs can reduce ecosystem degradation and enhance vegetation coverage, although where drought persists these programs have not worked well (Deng et al., 2014, Zhitao et al., 2014). Therefore, ecosystem water use efficiency

(WUE) is an important eco-physiological index which shows the relationship between carbon and ecosystem water cycles.

WUE is the main variable for understanding the impact of climate change on ecosystem productivity. Additionally, it is very essential to understand the linkage between the important biological processes of photosynthesis and transpiration, and the physical process of evaporation that together manage the Earth's carbon and water resources. Moreover, WUE can be used to point out the best strategy of water use in various ecosystems (Shaobo et al., Donovan and Ehleringer, 1991, Yu et al., 2008). It has been observed that WUE has a similar latitudinal trend on earth, increasing from the subtropics to about 51 N and then decreasing in higher latitudes (Tang et al., 2014). At the global scale, WUE varies with water availability with an increasing trend from moderate to extreme drought and a decreasing trend in wet conditions (Ponce-Campos et al., 2013). However, different ecosystem types have different sensitivity to changes of climatic conditions. At the ecosystem level, WUE is defined as the ratio between gross primary productivity (GPP) and evapotranspiration (ET) (Jassal et al., 2009, Brümmer et al., 2012). This definition was adopted in this study to make our findings comparable with previous studies (Reichstein, 2007, Huang et al., 2015, Yang et al., 2016a).

During the past decades, the spatiotemporal impacts of drought on WUE have been widely studied. Drought can also strongly affect the carbon cycle, composition, structure and function of the terrestrial ecosystem, which ultimately affect WUE (Breshears et al., 2005). The intensity and frequency of drought events have a significant increasing trend, which have a strong impact on WUE via the influence of carbon and water cycles. During the period of 2009-2010 in southwest China, there have been negative impacts of drought on vegetation in Yunnan, eastern Sichuan and Guizhou provinces which have resulted in the decline of primary productivity and carbon uptake (Li et al., 2019). Moreover, a serious drought in spring 2010 reduced the regional annual net and gross primary productivity of southwestern China to the lowest level by influencing the stomatal conductance, leaf area and net primary productivity, which eventually influenced WUE. However, it remains unclear how the severity of drought influences WUE (Ngugi et al., 2003). In addition, the strong coupling of carbon and water cycles revealed that any environmental disturbance on one component of WUE (i.e., GPP or ET) affects the other at the same time. WUE is influenced by environmental factors of precipitation, temperature, solar radiation, and ecosystem types. For example, under warm temperature, WUE decreases due to the sharp decrease in GPP. Precipitation affects the spatial and temporal variations of WUE, which can alter it by directly affecting the ecosystem evaporation and transpiration process while indirectly affecting the plant carbon uptake through soil water content regulation (Reichstein et al., 2010, Hu et al., 2010, Zhang et al., 2014, Tang et al., 2017). By contrast, increasing vapor pressure deficit leads to reduction in WUE of evergreen, rain, and deciduous forests (Law et al., 2002) and Douglas-Fir Stand (Stephane Ponton, 2006).

The objectives of this study are to analyze the spatiotemporal distribution of drought and ecosystem WUE in southwest China, and to explore the spatiotemporal responses of WUE to drought events during the period of 2001-2016. The findings from this study provide critical recommendations to governments and policy makers for implementing credible ecosystem and water resources management strategies under natural and human disturbances.

2. Material and methods

2.1 Study area and datasets

The study area covers 1.052×10^6 km^2 of southwest China comprising of Yunnan, Guizhou and Sichuan provinces. Topographically, the study area can be divided into three regions namely: western-Sichuan Plateau, Sichuan Basin, and Yunnan-Guizhou Plateau. The Sichuan basin is characterized by mountains with elevation varying between 1,000 and 3,000 m, the floor of the basin having an average elevation of 500 m. Yunnan-Guizhou plateau has an average elevation of 2,000 m (Figure 1a). The climate of the region is characterized as typical monsoonal but has temporarily fluctuated in the spatial distribution of the climate variables during the past decades. The annual precipitation decreased by 0.20 mm/year and temperature increased by 0.03 ^{0}C/year during the period from 1960 to 2016 (Mokhtar et al., 2020a).

To achieve our aim, we collected several datasets including climate, remotely sensed images (GPP, ET and ecosystem map) and topography (Digital Evaluation Model, DEM). Climate datasets of 103 meteorological stations (1960–2016) were obtained from China National Meteorological Data Sharing Platform (http://data.cma.cn/en). The products of GPP (MOD17A2H), ET (MOD16A2) and annual ecosystem map (MCD12Q1 V051), which were produced operationally for the southwest China's terrestrial surface using imagery from the MODIS (Moderate Resolution Imaging Spectroradiometer) sensor, with 500m spatial resolution for the period from 2001 to 2016 were used (earthdata.nasa.gov/). GPP was developed based on a light-use efficiency model and have been validated (Turner et al., 2006). The ecosystem systems were classified into 8 types as follows: deciduous forest, evergreen forest, mixed forest, shrub, savanna, wetland, agriculture and grass (Friedl et al., 2010).

The dominant ecosystem type is forest which occupies around 42% of the study area. Grass is the second major ecosystem type, occupying about 22% of the study area. Agriculture is the third major ecosystem type, covering about 20% of the study area (Table 1). Forest (evergreen, EF; deciduous, DF; mixed, MF) and grass ecosystem types are distributed primarily in the southern and eastern mountain areas, while grass dominates in the high mountains area (Sichuan plateau) and agriculture covers the basins area (Sichuan basin and some areas in Guizhou) (Figure 1). Agriculture is mainly rice, corn, grape, and flue-cured tobacco accounting for 18.87%, 16.83%, 22.25%, and 25.16% of the land area, respectively. Forest and agriculture increased by 77,896 km^2 and 2,334.8 km^2, respectively, during the period from 2001 to 2013, while grass and savanna decreased significantly by 23,029.7 km^2 and 28,802.5 km^2, respectively (Table 2). The grass area converted to forest was 22,404 km^2 (sum of row Grass under column EF, DF and MF) while the area converted from forest to grass was 11,462.9 km^2 as much (sum row EF, DF and MF under column Grass). The areas converted from agriculture to forest (43,940 km^2) were greater than that from forest to agriculture (25,921 km^2). The transition areas between forests and other ecosystem types were obviously greater than other transitions, particularly when compared with agriculture.

2.2 Drought characteristics

Various drought indices have been investigated including the Palmer Drought Severity Index (PDSI), the Soil Moisture Deficit Index (SMDI), standardized runoff index (SRI) and the Standardized Precipitation Index (SPI) (Shi, 2014, Hoover and Rogers, 2016). SPI is the most commonly used index to investigate drought categories (Núñez et al., 2014, Park et al., 2019). It has a simple structure and requires only rainfall data (Wang et al., 2015b, Xu et al., 2015). Therefore, it is more suitable for regions with limited hydrological data (Vergni and Todisco, 2011). Several studies have indicated that SPI is the major popular index for drought monitoring (Ma et al., 2018, Wu et al., 2007, Moradi et al., 2011, Nafarzadegan et al., 2012). Table 3 presents the categories of SPI that can be calculated for different timescales (i.e., 1, 3, 6, 9, 12 months) (Agnew, 2000). However, we restricted our study to only 3 (SPI-3) and 6 (SPI-6) months timescales which are considered representative of agricultural drought where rainfall shortage in a short time period is the main cause of drought (Park et al., 2018).

Drought variability in space and time was analyzed through principal component analysis (PCA) in S-mod and applied to both SPI-3 and SPI-6 (Rencher, 1998). PCA was applied to produce a smaller representative data, called the principal components (PCs), from the original one. Such a transformation is linear and depends on the eigenvectors of the covariance or correlation matrix (Xie et al., 2013). Then, Varimax orthogonal rotation methods were applied to the "loading" to capture subset regions affected by drought (Raziei et al., 2015). In this study, the dataset of SPI-3 and SPI-6 series were organized into a matrix with 684 rows (length of the monthly SPIs time series) and 103 columns (number of stations). PCA test was used to transform the SPI series (90 stations) into PCs to produce more localized spatial regions. The Varimax orthogonal rotation method was applied to the "loadings" because it simplifies the structure of the patterns by forcing the value of the loading coefficients towards zero or within ± 1 (Tian and Quiring, 2019, Raziei et al., 2009). The S-mode of the PCA was calculated for SPI-3 and SPI-6 to define the spatial patterns of drought variability in the study area.

Several methods have been widely used for drought event identification including the threshold level method, run theory, and empirical orthogonal functions (Lloyd-Hughes, 2012). In this study we determined a drought event as a period in which the SPI is continuously negative (Tan et al., 2015a, McKee et al., 1993), i.e., for all SPI < 0. To further discriminate drought impacts on the regional ecosystem, the areas affected by drought were estimated based on Table 3, and were identified using Eq. (1) as (Agnew, 2000, Tan et al., 2015a):

$$SEoD \quad (\%) = \frac{m}{M} \times 100 \tag{1}$$

where SEoD is the spatial drought extent, m is the number of drought points (SPI < 0), and M is the total number of points in the study area. Eq. (1) highlights the susceptibility of areas to different drought categories. The drought-prone areas were examined by the percentage of the number of drought locations in the total study area for the different drought categories.

Once a specific drought event was identified, the drought characteristics of duration (DD), intensity (DI), and severity (DS) were analyzed. DD is the number of months in which SPI values are negative for a drought event (Spinoni et al., 2014, Guo et al., 2017) and DS is the absolute sum of the SPI values during a drought event calculated as:

$$DS = \left| \sum_{i=1}^{DD} SPI_i \right| \tag{2}$$

where SPI_i is the SPI value for month i and DI is the lowest SPI value during the specific drought event. Therefore**,** the total duration of a drought episode (TDD) is defined as either the sum of the number of continuous months n_i when SPI < 0 (Spinoni et al., 2014, Guo et al., 2017) as:

$$TDD(\%) = \sum \frac{n_i}{N_i} \times 100 \tag{3}$$

where n_i is the sum of months encompassing drought episodes, N_i is the total studied period in months for each station.

2.3 WUE analysis

Monthly WUE was calculated as the ratio between GPP and ET for each month during the period of 2001–2016 for each grid cell of the study area as:

$$WUE = \frac{GPP}{ET} \tag{4}$$

where WUE is in g $Ckg^{-1}H_2O$, GPP is in g Cm^{-2} and ET is in kg H_2O m^{-2}.

Drought events during the period of 2001-2016 were first identified. Next, we calculated the difference between the WUE of the drought year and that of a normal year (ΔWUE). WUE exhibits positive anomalies and drought is likely to increase WUE when the ΔWUE value is greater than 0 while WUE shows negative anomalies when the ΔWUE value is less than 0. Mann–Kendall (M-K) and Sen's slope test were applied to determine the linear trend of monthly WUE, SPIs (SPI-3 and SPI-6) and the climate variables. The M-K test has been recommended for analysis of trends in timeseries of precipitation, temperature, runoff, and water quality (Mokhtar et al., 2020b, Mokhtar et al., 2020a). Pearson correlation analysis was applied to study the impact of drought on the monthly WUE for each ecosystem type in order to identify the positive and negative effects of drought on ecosystem WUE for each grid cell over the study area.

3. Results

3.1 Spatial and temporal variations of droughts over the past decades

Southwest China has suffered from serious droughts that have significantly affected ecosystem production and WUE. In order to identify the drought episodes in southwest China, SPI-3 and SPI-6 were analyzed for 103 stations using the M-K test. The results showed that, for SPI-3, there were positive significant trend for 38 stations (36.9%, $p<0.05$), with 22 of them mainly in the Guizhou province having a p-value < 0.001 (Figure 2). Sixty-five stations that showed no trend were concentrated in the Yunnan and the eastern part of Sichuan and Guizhou provinces. For SPI-6, a significant trend ($p<0.05$) was found in 62 stations (60%) which covered a large area of southwest China, and 33 stations (32%) with $p <0.001$. The SPI-3 in the northwest of Sichuan province had a positive significant trend with Sen's slope values that ranged from 0.0004 to 0.0009 (Figure 2), being the same results for SPI-6. The PCs were retained for Varimax rotation in order to identify the 18 sub-regions of SPI-3 and SPI-6 by applying scree plots to identify the number of PCs to retain (Hair Jr, 1999). Figure 2c-d show a slight change in slope at the eigenvalues, although there is a smaller change for SPI-6 compared with SPI-3. These eigenvalues for the SPIs were used to determine the contribution of the dataset variance of each factor, cumulatively and individually. Accordingly, we defined eighteen components that explained about 72.8% of the total variance of SPI-3 and 71.9% for SPI-

6, the remaining components accounting for the remaining variance. The loadings corresponding to each PC were mapped to show the spatial patterns of drought variability across the studied area (Alsafadi et al., 2020). The results illustrate the spatial distribution of the loadings corresponding to each extracted component. The spatial pattern shows distinct areas with high heterogeneity in wet and dry events due to the large area that extend across hundreds of kilometers, with several climate patterns influenced by atmospheric circulation and general distribution of rainfall. For example, PC1 of SPI-3 timescale corresponds to the southern region with high annual precipitation (1000-1500 mm), i.e., temperate climate without dry season, while PC2 mainly follows a temperate climate with dry winter experiencing total annual rainfall in excess of 2000 mm. In the same context, PC4 reflects drought variability in the northern regions with moderate precipitation (500-700 mm). Spatially, the PCs suggest high heterogeneity of drought in the study area. Thus, the heterogeneity reflects the complex interactions among the region's topography, atmospheric circulation scale processes, monsoon flow, and anthropogenic forcing.

Furthermore, the SPI-3 and SPI-6 results indicated that a significant change occurred after 2009 in southwest China (Fig. 3). The proportion of the drought area in southwest China was used to measure the spatial extent of drought. Approximately 20% of the total area affected was subjected to extreme droughts for SPI-3 and SPI-6. However, more than 30% of the total area was categorized as moderate drought which is similar to the observation by (Liu et al., 2014) over China (Figure 4). In order to study the drought events after 2000, six seasons (autumn 2006, autumn 2009, winter 2010, summer 2011, autumn 2011 and winter 2013) were identified among the 64 seasons for the period of

2001-2016. The highest number of the total drought durations happened in the southern part of the study area, especially in central Yunnan province that reached 90% (> 50 months) of the total period. Moreover, the results of SPI-6 indicated longer durations of drought than SPI-3, especially in the Yunnan province. The highest severity was recorded in the eastern part of Yunnan and the lowest values in the northern part of Sichuan province (Figure 5). The drought intensity ranged from -3 to less than -1 over the study area, the highest intensity occurring in the southeast of Yunnan province.

3.2 Spatiotemporal variations of water use efficiency (WUE)

WUE fluctuated temporally and spatially based on the drought situation and the environmental factors. The average annual WUE was 2.37 gC/kgH_2O for the period from 2001 to 2016, with the highest value registered in 2001 (3.99 gC/kgH_2O) and the lowest value in 2004 (1.38 gC/kgH_2O). The annual WUE shows a decreasing linear trend of -0.05 gC/kgH_2O/year. GPP and ET increased by 0.63 gC/year and 5.82 kgH_2O/year, respectively, which are consistent with the increasing trend of temperature and solar radiation. The annual pattern of WUE by location depicts a long-term change in the ecosystem types. WUE reached 5.6 gC/kgH_2O for the forest ecosystem in most of Yunnan and Guizhou provinces, and averaged at 1.2 gC/KgH_2O for the grass ecosystem in the northern Sichuan.

Seasonally, WUE had the lowest value for grasses located in the northwest of Sichuan province in the winter season. However, the northeastern part of Sichuan province had a high WUE where agricultural activities were prominent. By contrast, the highest values of 5 gC/kgH_2O occurred in the forest ecosystem of southern Yunnan province. The summer season recorded the highest values of WUE (> 10 gC/kgH_2O) in comparison with the other seasons, especially in Yunnan province (>20 gC/kgH_2O). For spring and autumn seasons, the highest WUE values were located in the east of Guizhou and the south of Yunnan, respectively. However, the northwest of Sichuan has the lowest values in spring and autumn seasons. In terms of ecosystem types, the average annual WUE values (gC kg^{-1} H_2O) were in the following decreasing order; evergreen broadleaf forests (2.32) > mixed forests (2.02) > savannas (1.83), and the lowest ecosystem WUE was in grass (0.95) (Figure 5). Our findings indicated that the WUE ecosystem types varied over time and location due to the significant variations of the climate variables.

Since WUE depends on GPP and ET, it is expected that climate factors that affect GPP and/or ET should also affect WUE. While GPP and ET both increased during the study period, WUE showed a decreasing trend in the same period because the rate of increase in ET was higher than in GPP. Increasing solar radiation amount, vapor pressure deficit, temperature and precipitation contributed to increases in GPP by 0.47, 3.9, 4.3 and 0.33 gC/m^2, and in ET by 0.15, 1.2, 1.3 and 0.1 kgH_2O, respectively (Figure 6). Temperature is the main factor controlling the annual and monthly GPP and ET, which eventually leads to a decrease in WUE. Solar radiation and vapor pressure deficit had a positive impact on WUE with a slope of 0.002 and 0.001 gC/kH_2O per year, respectively.

3.3 Responses of WUE to drought

The monthly correlation coefficient between the SPIs and WUE shows a significant spatial heterogeneity that ranged from -0.4 to 0.6. For SPI-3 and in the winter season, WUE had the highest positive significant correlation with drought (26%, $p<0.05$) in

Yunnan province and some other parts of the south Sichuan and Guizhou provinces. Nonetheless, the non-significant positive correlation was more than 57% of the total area in the autumn season. By contrast, the significant negative correlation with drought was 8.6% (non-significant in 58%, $p< 0.05$) which covered the whole of Guizhou province. For SPI-6, WUE had a positive significant correlation with drought of 35.5% (non-significant in 63%, $p< 0.05$) over the whole study area except small pockets in the northwest of Yunnan and the northeast of Guizhou province during the winter season (Figure 7). However, the negative correlation with SPI-6 was significant in 11% and non-significant in 50% of the total area that covered Yunnan and Guizhou and the north of Sichuan province (Table 4). In the summer season, the WUE had a negative correlation with SPIs due to the abundant precipitation in summer season that leads to increase in WUE through a higher rate of increase in GPP than in ET. In terms of ecosystem types, WUE had a correlation with SPI-3 of -0.37 for agriculture in the summer season (JJA), while in the winter season (DJF) it was 0.26 with evergreen needle-leaf forests (ENF) (Figure 8). By contrast, the WUE presented negative correlation with SPI-3 for agriculture in autumn (SON) was -0.20. For SPI-6, in summer season, evergreen broad-leaf forests (EBF) and agriculture had a positive correlation of 0.39 and 0.35, respectively. Likewise, ENF had a positive correlation of 0.42 and grass was -0.10 with WUE in the winter season (Figure 8).

Six drought events (autumn 2006, autumn 2009, winter 2010, summer 2011, autumn 2011 and winter 2013) were identified during the period of 2001-2016 based on the average WUE values. The ΔWUE was used to study the impacts of drought on the ecosystems. Figure 9 shows the spatial distribution of WUE for the drought seasons and the spatial patterns of the annual WUE anomalies. For example, the spatial distribution of WUE and the total average in autumn 2009 (Figure 9b) changed significantly, and this is also true for summer 2011 (Figure 9e). ∆WUE in autumn 2009 and summer 2011 were the highest decrease in values by -82% and -88%, respectively (Figure 9k and m). By contrast, ∆WUE in autumn 2006 and winter 2013 were the highest increase in values by 60% and 33%, respectively. In autumn 2006, the drought event had a significant positive effect on WUE for more than 80% of the ecosystem grid cells of forest, shrubland, savanna and agriculture ecosystems (Figure 9j). In winter 2010, the drought had significant negative impacts on more than 65% of ecosystem type grid cells except for the grass ecosystem that showed a positive increase for all grid cells (Table 5).

Finally, the spatial extent of drought (SEoD) areas during the period from 2009 to 2013 were analyzed to determine the responses of the ecosystems' WUE, GPP and ET to drought areas at the seasonal scale (Figure 10). WUE has slightly positively correlated with the percentage drought area for the SPIs. Moreover, the highest WUE values were in spring 2010 whereas the highest drought area was in winter 2010, indicating that the impact of the previous drought season on WUE was higher than the current season (Figure 10a). The impacts of drought on GPP and ET were similar. Thus, the variations in seasonal WUE were mainly caused by the variations in seasonal values of GPP and ET.

4. Discussion

The characteristics of climatic change in southwest China indicate that temperature exhibits an increasing trend while precipitation has a decreasing trend. The significant reduction of sunshine in southwest China plays a vital role in the evaporation rate that is responsible for the drought events (Mokhtar et al., 2020a). The significant positive correlation between GPP and ET during the 16 years (2001-2016) were lower than reported by previous investigations (Krishnan et al., 2006, Yu et al., 2008, Jassal et al., 2009) for the different ecosystem types. Lower WUE in the mixed forest plantation is attributed to the broadleaf dominant stand with higher evapotranspiration and lower GPP. For example, in the dry season, GPP and ET drop gradually due to decline in air temperature, and in February and March GPP and ET continue to drop to reach the lowest values. Thus, WUE decreased by 0.8 gC/kgH_2O (27% of the annual average) during the study period, responding to the variations of drought and environmental factors. This result corroborates the findings of (Xue et al., 2015). By contrast, the highest values of WUE occurred in July and August, which also agree with the investigation of (Tong et al., 2014). This could be due to the stoma closing during high temperature, decreasing transpiration rate more than the photosynthesis rate, which results in the rise of WUE in the wet season (Maroco et al., 1997, Brümmer et al., 2012). Moreover, the spatial differences of WUE were influenced by climate conditions and plant morphology, this result being consistent with those of Yang et al. (2016), Huang et al. (2017), and Xue et al. (2015). The annual WUE of southwestern China was higher than the mean annual WUE of China's terrestrial ecosystems (Liu et al., 2015a), and the global WUE (Ito, .2012). WUE correlated positively with SPI-3 and SPI-6 over Yunnan province in spring and summer seasons. The result of Yang et al. (2016) (Yang et al., 2016b)(Yang et al., 2016b)(Yang, Guan et al. 2016)(Yang et al., 2016b) is consistent with our finding (Yang et al., 2016a). In the dry season WUE responded negatively to increasing SPI-3 and SPI-6 as observed by Guo et al. (2019). Table 6 illustrates the correlation coefficient between WUE and the environmental factors for the ecosystem types, all being positive except for the evergreen broadleaf forests and the savanna ecosystem. This explains the difference between tropical and temperate ecosystems, and as reported by (Tian et al., 2010). Moreover, precipitation had a strong positive correlation between WUE and the evergreen broadleaf forest (0.87), deciduous broadleaf forest (0.82) and grass ecosystem (0.85). Precipitation is one of the major important factors for WUE because it controls the evaporation rate. Meanwhile, increased precipitation can contribute to increase in canopy cover and a decrease in soil evaporation, contributing to an increase in WUE. Also, increase precipitation leads to increase in GPP and ET. In the wet season, precipitation is not the main limiting factor for ecosystem growth and WUE, as the shortwave solar radiation and vapor pressure deficit are the limiting factors by controlling transpiration and photosynthesis. Further, photosynthesis is limited under strong solar radiation and vapor pressure deficit which is reflected on WUE. This result is inconsistent with the findings of (Beer et al., 2009, Xin et al., 2016, Wagle et al., 2016). Solar radiation controls transpiration and photosynthesis and there is a significant correlation between solar radiation and WUE for deciduous needleleaf forest (0.82), deciduous broadleaf forest (0.78) and evergreen broadleaf forest (0.74). Mean air temperature has both positive and negative effect on WUE at the annual and seasonal scale due to its complex impact on both GPP and ET through the influence of LAI (leave area index) that increases ET especially in the subtropical ecosystems (Tan et al., 2015b).

Previous studies have indicated both positive and negative correlation between WUE and drought (Yang et al., 2016b, Guo et al., 2019). The variations could be due to the numerous drought indices, locations, and data sources used. Furthermore, the differences in sensitivities of GPP and ET to drought control the WUE-drought relationships across various sub-regions and ecosystems (Liu et al., 2015b, Yang et al., 2016b). For example, water resources played a vital role for ecosystem productivity (Bai et al., 2008). Sichuan province has a sparse ecosystem (e.g., grass, agriculture and forest), thus, increasing precipitation would alleviate water shortages and improve gross primary productivity. In this study, the ecosystem types indicated different WUE that presented different responses to drought due to the differences in sensitivities of GPP and ET to climate change, resulting in variabilities in carbon uptake and water consumption (Liu et al., 2013b, Knapp and Smith, 2001). For instance, grass ecosystem yielded the lowest WUE but had a significant positive correlation with SPI due to their growth, activity and productivity that depend strongly on water supply (Ponce-Campos et al., 2013, Knapp and Smith, 2001). However, the WUE of agriculture in wetter regions had a positive response to drought because of their sensitivity to water shortages. The crops would wilt or even die under water deficient conditions, thus WUE will decrease with increase in ET and decline in ecosystem GPP (Liu et al., 2013a, Liu et al., 2013b). In semi-humid regions with abundant vegetation (i.e., grass, DBF, DNF and MF), energy is the major influence on ecosystem growth during drought periods because the incoming shortwave solar radiation is reduced which results in obstructing the absorption of carbon (Liu et al., 2015b). Generally, the shortage in precipitation and lack of cloud cover result in drought because of increase in incoming solar radiation for the ecosystem processes (GPP and ET) to accelerate (Larcher, 2003). The negative correlation coefficient between drought and ET was greater than between drought and GPP, resulting in a decrease in annual WUE as also reported by (Liu et al., 2015a). The overall sensitivity of GPP and ET to drought index is low in both dry and wet ecosystems, but ET is sensitive to changes in hydro-climatic conditions. Therefore, it is the primary reason for the negative correlation between WUE and SPI which indicates that it is not only SPI that controls WUE. Another reason is that drought and changes in WUE may not occur at the same time because of the different impact of drought on carbon uptake and water loss.

5. Conclusions

In this paper we analyzed the monthly spatiotemporal patterns of WUE and its response to drought using MODIS data products (GPP and ET) and the SPI-3 and SPI-6 drought indices in southwest China during the period of 2001–2016. The PCs present a high spatial heterogeneity of drought in the study area. The main conclusions are the following.

- Six drought events (autumn 2006, autumn 2009, winter 2010, summer 2011, autumn 2011 and winter 2013) were identified during the period of 2001-2016.
- The monthly correlation coefficient between the SPIs and WUE exhibits a large spatial heterogeneity, especially in the summer season when the WUE is negatively correlated with the drought indices (SPI-3/SPI-6). The highest and lowest annual WUE were recorded for the evergreen broadleaf forest and grass ecosystem, respectively.

- The highest decreasing changes in WUE occurred during autumn 2009 and summer 2011, whereas WUE for autumn 2006 and winter 2013 showed the highest increasing values. WUE is expected to continue changing under future climate change, particularly as drought is projected to increase in both frequency and severity.

Our findings have implications for ecosystem management and climate policy making. Moreover, it can help to better understand plant water use strategy in order to implement feasible water use strategies to minimize the influence of drought under the warming climate.

Acknowledgements: The research work of this article was financially supported by Projects of the Second Tibetan Plateau Scientific Expedition and Research Program (Grant SQ2019QZKK2003), the National Key Research and Development Program (Grant No. 2017YFC0505200; 2017YFC0505205), the National Natural Science Foundation of China (Grant No. 41672180), Science & Technology Basic Resources Investigation Program of China (Grant No. 2017FY101303), the Strategic Priority Research Program of the Chinese Academy of Sciences (Grant No. XDA23020603), the Science & Technology Basic Resources Investigation Program of China (Grant No. 2017FY101303), the Project of the Integrated Scientific Expedition of the Ailao-Wuliang Mountains National Park (Grant No. 2019IB018); the Guangdong Rural Science and Technology Commissioner Project (Grant No. 319B0203) of China, Key Platforms and Scientific Research Projects in Universities in Guangdong Province of China (Grant No. 2018KTSCX212).

Author Contributions: AM and KA collected the research data, analyzed the data and prepared the draft of the manuscript. AM, KA, YGA and HH designed the research and provided suggestions to data analysis. AM, KA and HZ generated the figures. WH and YL helped in the revision work. All authors read and edited the manuscript.

Conflicts of interest: The authors declare no conflicts of interest.

Data Availability Statement: The data that support the findings of this study are available from the corresponding author upon reasonable request.

References

AGNEW, C. 2000. Using the SPI to identify drought.

ALSAFADI, K., MOHAMMED, S., AYUGI, B., SHARAF, M. & HARSÁNYI, E. 2020. Spatial–Temporal Evolution of Drought Characteristics Over Hungary Between 1961 and 2010. *Pure and Applied Geophysics*, 1-18.

BAI, Y., WU, J., XING, Q., PAN, Q., HUANG, J., YANG, D. & HAN, X. 2008. Primary production and rain use efficiency across a precipitation gradient on the Mongolia plateau. *Ecology,* 89, 2140-2153.

BEER, C., CIAIS, P., REICHSTEIN, M., BALDOCCHI, D., LAW, B. E., PAPALE, D., SOUSSANA, J. F., AMMANN, C., BUCHMANN, N. & FRANK, D. 2009. Temporal and among‐site variability of inherent water use efficiency at the ecosystem level. *Global Biogeochemical Cycles,* 23, GB2018.

BRESHEARS, D. D., COBB, N. S., RICH, P. M., PRICE, K. P., ALLEN, C. D., BALICE, R. G., ROMME, W. H., KASTENS, J. H., FLOYD, M. L., BELNAP, J., ANDERSON, J. J., MYERS, O. B. & MEYER, C. W. 2005. Regional vegetation die-off in response to global-change-type drought. *Proc Natl Acad Sci U S A,* 102, 15144-8.

BRÜMMER, C., BLACK, T. A., JASSAL, R. S., GRANT, N. J., SPITTLEHOUSE, D. L., CHEN, B., NESIC, Z., AMIRO, B. D., ARAIN, M. A. & BARR, A. G. 2012. How climate and vegetation type influence evapotranspiration and water use efficiency in Canadian forest, peatland and grassland ecosystems. *Agricultural & Forest Meteorology,* 153, 14-30.

DENG, L., SHANGGUAN, Z. P. & SWEENEY, S. 2014. "Grain for Green" driven land use change and carbon sequestration on the Loess Plateau, China. *Scientific Reports,* 4, 7039.

DONOVAN, L. A. & EHLERINGER, J. R. 1991. Ecophysiological differences among juvenile and reproductive plants of several woody species. *Oecologia,* 86**,** 594-597.

FRIEDL, M. A., SULLA-MENASHE, D., TAN, B., SCHNEIDER, A., RAMANKUTTY, N., SIBLEY, A. & HUANG, X. 2010. MODIS Collection 5 global land cover: Algorithm refinements and characterization of new datasets. *Remote Sensing of Environment,* 114**,** 168-182.

GUO, H., BAO, A., LIU, T., FELIX, N., HE, D., ALISHIR, K. & PHILIPPE, D. M. 2017. Meteorological Drought Analysis in the Lower Mekong Basin Using Satellite-Based Long-Term CHIRPS Product. *Sustainability,* 9**,** 901.

GUO, L., SUN, F., LIU, W., ZHANG, Y., WANG, H., CUI, H., WANG, H., ZHANG, J. & DU, B. 2019. Response of ecosystem water use efficiency to drought over China during 1982–2015: Spatiotemporal variability and resilience. *Forests,* 10**,** 598.

HAIR JR, J. 1999. Multivariate Data Analysis with Readings. 4th ed1995. Englewood Cliffs, NJ: Prentice Hall.

HOOVER, D. L. & ROGERS, B. M. 2016. Not all droughts are created equal: the impacts of interannual drought pattern and magnitude on grassland carbon cycling. *Global Change Biology,* 22**,** 1809-1820.

HU, Z. M., YU, G. R., FAN, J. W., ZHONG, H. P., WANG, S. Q. & LI, S. G. 2010. Precipitation-use efficiency along a 4500-km grassland transect. *Global Ecology & Biogeography,* 19**,** 842-851.

HUANG, M., PIAO, S., SUN, Y., CIAIS, P., CHENG, L., MAO, J., POULTER, B., SHI, X., ZENG, Z. & WANG, Y. 2015. Change in terrestrial ecosystem water-use efficiency over the last three decades. *Glob Chang Biol,* 21**,** 2366-78.

ITO, A., & INATOMI, M. .2012. Water-use efficiency of the terrestrial biosphere: a model analysis focusing on interactions between the global carbon and water cycles. . *Journal of Hydrometeorology, ,* 13**,** 681-694.

JASSAL, R. S., BLACK, T. A., SPITTLEHOUSE, D. L., BRÜMMER, C. & NESIC, Z. 2009. Evapotranspiration and water use efficiency in different-aged Pacific Northwest Douglas-fir stands. *Agricultural & Forest Meteorology,* 149**,** 1168-1178.

KNAPP, A. K. & SMITH, M. D. 2001. Variation among biomes in temporal dynamics of aboveground primary production. *Science,* 291**,** 481-484.

KRISHNAN, P., BLACK, T. A., GRANT, N. J., BARR, A. G., HOGG, E. H., JASSAL, R. S. & KAI, M. 2006. Impact of changing soil moisture distribution on net ecosystem productivity of a boreal aspen forest during and following drought. *Agricultural & Forest Meteorology,* 139**,** 208-223.

LARCHER, W. 2003. *Physiological plant ecology: ecophysiology and stress physiology of functional groups*, Springer Science & Business Media.

LAW, B. E., FALGE, E., GU, L., BALDOCCHI, D. D., BAKWIN, P., BERBIGIER, P., DAVIS, K., DOLMAN, A. J., FALK, M. & FUENTES, J. D. 2002. Environmental controls over carbon dioxide and water vapor exchange of terrestrial vegetation. *Agric for Meteorol,* 113**,** 97-120.

LI, X., LI, Y., CHEN, A., GAO, M., SLETTE, I. J. & PIAO, S. 2019. The impact of the 2009/2010 drought on vegetation growth and terrestrial carbon balance in Southwest China. *Agricultural and Forest Meteorology,* 269**,** 239-248.

LIU, Y., JU, W., HE, H., WANG, S., SUN, R. & ZHANG, Y. 2013a. Changes of net primary productivity in China during recent 11 years detected using an ecological model driven by MODIS data. *Frontiers of Earth Science,* 7**,** 112-127.

LIU, Y., XIAO, J., JU, W., ZHOU, Y., WANG, S. & WU, X. 2015a. Water use efficiency of China's terrestrial ecosystems and responses to drought. *Sci Rep,* 5**,** 13799.

LIU, Y., XIAO, J., JU, W., ZHOU, Y., WANG, S. & WU, X. 2015b. Water use efficiency of China's terrestrial ecosystems and responses to drought. *Scientific reports,* 5**,** 1-12.

LIU, Y., ZHOU, Y., JU, W., CHEN, J., WANG, S., HE, H., WANG, H., GUAN, D., ZHAO, F. & LI, Y. 2013b. Evapotranspiration and water yield over China's landmass from 2000 to 2010. *Hydrology and Earth System Sciences,* 17**,** 4957.

LIU, Y., ZHOU, Y., JU, W., WANG, S., WU, X., HE, M. & ZHU, G. 2014. Impacts of droughts on carbon sequestration by China's terrestrial ecosystems from 2000 to 2011. *Biogeosciences,* 11**,** 2583.

LLOYD‐HUGHES, B. 2012. A spatio‐temporal structure‐based approach to drought characterisation. *International Journal of Climatology,* 32**,** 406-418.

MA, F., LUO, L., YE, A. & DUAN, Q. 2018. Seasonal drought predictability and forecast skill in the semi-arid endorheic Heihe River basin in northwestern China. *Hydrology & Earth System Sciences,* 22**,** 5697-5709.

MAROCO, J. P., PEREIRA, J. S. & CHAVES, M. M. 1997. Stomatal Responses to Leaf-to-Air Vapour Pressure Deficit in Sahelian Species. *Functional Plant Biology,* 24**,** 381-387.

MCKEE, T. B., DOESKEN, N. J. & KLEIST, J. The relationship of drought frequency and duration to time scales. Proceedings of the 8th Conference on Applied Climatology, 1993. Boston, 179-183.

MOKHTAR, A., HE, H., ALSAFADI, K., LI, Y., ZHAO, H., KEO, S., BAI, C., ABUARAB, M., ZHANG, C., ELBAGOURY, K., WANG, J. & HE, Q. 2020a. Evapotranspiration as a response to climate variability and ecosystem changes in southwest, China. *Environmental Earth Sciences,* 79**,** 312.

MOKHTAR, A., HE, H. M., ZHAO, H. F., KEO, S., BAI, C. Y., ZHANG, C. J., MA, Y., IBRAHIM, A., LI, Y., LI, F. J., HE, W. M., ABDO, A. I. & ZHOU, J. 2020b. Risks to water resources and development of a management strategy in the river basins of the Hengduan Mountains, Southwest China. *Environmental Science-Water Research & Technology,* 6**,** 656-678.

MOKHTAR, A., JALALI, M., ELBELTAGI, A., AL-ANSARI, N., ALSAFADI, K., ABDO, H. G., SAMMEN, S. S., GYASI-AGYEI, Y., RODRIGO-COMINO, J. & HE, H. 2021. Estimation of SPEI Meteorological Drought using Machine Learning Algorithms. *IEEE Access*.

MORADI, H. R., RAJABI, M. & FARAGZADEH, M. 2011. Investigation of meteorological drought characteristics in Fars province, Iran. *Catena,* 84**,** 35-46.

MU, Q., ZHAO, M., RUNNING, S. W., LIU, M. & TIAN, H. 2015. Contribution of increasing CO2 and climate change to the carbon cycle in China's ecosystems. *Journal of Geophysical Research Biogeosciences,* 113**,** n/a-n/a.

NAFARZADEGAN, A. R., ZADEH, M. R., KHERAD, M., AHANI, H., GHAREHKHANI, A., KARAMPOOR, M. A. & KOUSARI, M. R. 2012. Drought area monitoring during the past three decades in Fars province, Iran. *Quaternary International,* 250**,** 27-36.

NARASIMHAN & SRINIVASAN 2005. Development and evaluation of Soil Moisture Deficit Index (SMDI) and Evapotranspiration Deficit Index (ETDI) for agricultural drought monitoring. *Agricultural & Forest Meteorology,* 133**,** 0-88.

NGUGI, M. R., HUNT, M. A., DOLEY, D., RYAN, P. & DART, P. J. 2003. Effects of soil water availability on water use efficiency of Eucalyptus cloeziana and Eucalyptus argophloia plants. *Australian Journal of Botany,* 51**,** 159-166.

NÚÑEZ, J., RIVERA, D., OYARZÚN, R. & ARUMÍ, J. 2014. On the use of Standardized Drought Indices under decadal climate variability: Critical assessment and drought policy implications. *Journal of Hydrology,* 517**,** 458-470.

PARK, J., LIM, Y.-J., KIM, B.-J. & SUNG, J. H. 2018. Appraisal of drought characteristics of representative drought indices using meteorological variables. *KSCE Journal of Civil Engineering,* 22**,** 2002-2009.

PARK, J., SUNG, J. H., LIM, Y.-J. & KANG, H.-S. 2019. Introduction and application of non-stationary standardized precipitation index considering probability distribution function and return period. *Theoretical and Applied Climatology,* 136**,** 529-542.

PONCE-CAMPOS, G. E., MORAN, M. S., HUETE, A., ZHANG, Y., BRESLOFF, C., HUXMAN, T. E., EAMUS, D., BOSCH, D. D., BUDA, A. R. & GUNTER, S. A. 2013. Ecosystem resilience despite large-scale altered hydroclimatic conditions. *Nature,* 494**,** 349-352.

QUERE, C. L., RAUPACH, M. R., CANADELL, J. G., MARLAND, G., BOPP, L., CIAIS, P., CONWAY, T. J., DONEY, S. C., FEELY, R. A. & FOSTER, P. 2012. *Trends in the sources and sinks of carbon dioxide*.

RAZIEI, T., MARTINS, D. S., BORDI, I., SANTOS, J. F., PORTELA, M. M., PEREIRA, L. S. & SUTERA, A. 2015. SPI modes of drought spatial and temporal variability in Portugal: Comparing observations, PT02 and GPCC gridded datasets. *Water resources management,* 29**,** 487-504.

RAZIEI, T., SAGHAFIAN, B., PAULO, A. A., PEREIRA, L. S. & BORDI, I. 2009. Spatial patterns and temporal variability of drought in western Iran. *Water Resources Management,* 23**,** 439.

REICHSTEIN, M., CIAIS, P., PAPALE, D., VALENTINI, R., RUNNING, S., VIOVY, N., ET AL. 2007. Reduction of ecosystem productivity and respiration during the European summer 2003 climate anomaly: a joint flux tower, remote sensing and modelling analysis. . *Global Change Biology,* 13**,** 634–651.

REICHSTEIN, M., TENHUNEN, J. O., OURCIVAL, J. M. & RAMBAL, S. 2010. Severe drought effects on ecosystem CO2 and H2O fluxes at three Mediterranean evergreen sites: revision of current hypotheses? [Review]. *Global Change Biology,* 8**,** 999-1017.

RENCHER, A. C. 1998. *Multivariate statistical inference and applications,* Wiley New York.

SHAOBO, S., ZHAOLIANG, S., XIUCHEN, W., TIEJUN, W., YUNTAO, W., WENLI, D., TAO, C., CHUNLIN, H., XUEJUN, Z. & BO, P. Spatio-temporal variations in water use efficiency and its drivers in China over the last three decades. *Ecological Indicators*.

SHEFFIELD, J. & WOOD, E. F. 2008. Projected changes in drought occurrence under future global warming from multi-model, multi-scenario, IPCC AR4 simulations. *Climate Dynamics,* 31**,** 79-105.

SHEFFIELD, J., WOOD, E. F. & RODERICK, M. L. 2012. Little change in global drought over the past 60 years. *Nature,* 491**,** 435-438.

SHI, Z., THOMEY, M. L. , MOWLL, W. , LITVAK, M. , BRUNSELL, N. A. , & COLLINS, S. L. , ET AL. 2014. Differential effects of extreme drought on production and respiration: synthesis and modeling analysis. . *Biogeosciences, ,* 11**,** 621-633.

SPINONI, J., NAUMANN, G., CARRAO, H., BARBOSA, P. & VOGT, J. R. 2014. World drought frequency, duration, and severity for 1951–2010. *International Journal of Climatology,* 34.

STEPHANE PONTON, F., L. B. , ALSTAD, K. P. , JOHNSON, B. G. , & BARR, A. G. 2006. Comparison of ecosystem water-use efficiency among douglas fir forest, aspen forest and grassland using eddy covariance and carbon isotope techniques. . *Global Change Biology,* 12.

TAN, C., YANG, J. & LI, M. 2015a. Temporal-spatial variation of drought indicated by SPI and SPEI in Ningxia Hui Autonomous Region, China. *Atmosphere,* 6**,** 1399-1421.

TAN, Z., ZHANG, Y. I., DENG, X., SONG, Q. & YANG, L. A. 2015b. Interannual and seasonal variability of water use efficiency in a tropical rainforest: Results from a 9-year eddy flux time series. *Journal of Geophysical Research Atmospheres,* 120**,** 464-479.

TANG, X., LI, H., DESAI, A. R., NAGY, Z., LUO, J., KOLB, T. E., OLIOSO, A., XU, X., YAO, L. & KUTSCH, W. 2014. How is water-use efficiency of terrestrial ecosystems distributed and changing on Earth? *Sci Rep,* 4**,** 7483.

TANG, X., LI, H., MA, M., YAO, L., PEICHL, M., ARAIN, A., XU, X. & GOULDEN, M. 2017. How do disturbances and climate effects on carbon and water fluxes differ between multi-aged and even-aged coniferous forests? *Science of the Total Environment,* 599-600, 1583.

TIAN, H., CHEN, G., LIU, M., CHI, Z., GE, S., LU, C., XU, X., WEI, R., PAN, S. & CHAPPELKA, A. 2010. Model estimates of net primary productivity, evapotranspiration, and water use efficiency in the terrestrial ecosystems of the southern United States during 1895–2007. *Forest Ecology & Management,* 259, 1311-1327.

TIAN, L. & QUIRING, S. M. 2019. Spatial and temporal patterns of drought in Oklahoma (1901–2014). *International Journal of Climatology,* 39, 3365-3378.

TONG, X., ZHANG, J., MENG, P., LI, J. & ZHENG, N. 2014. Ecosystem water use efficiency in a warm-temperate mixed plantation in the North China. *Journal of Hydrology,* 512, 221-228.

TRENBERTH, K. E., DAI, A., SCHRIER, G. V. D., JONES, P. D., BARICHIVICH, J., BRIFFA, K. R. & SHEFFIELD, J. 2013. Global warming and changes in drought. *Nature Climate Change,* 4, 17-22.

TURNER, DAVID, P., RITTS, WILLIAM, D., COHEN, WARREN, B., GOWER, STITH, T. & STEVE, W. 2006. Evaluation of MODIS NPP and GPP products across multiple biomes. *Remote Sensing of Environment,* 102, 282-292.

VERGNI, L. & TODISCO, F. 2011. Spatio-temporal variability of precipitation, temperature and agricultural drought indices in Central Italy. *Agricultural & Forest Meteorology,* 151, 301-313.

VICENTE-SERRANO, S. M., GERARD, V. D. S. , BEGUERÍA, SANTIAGO, AZORIN-MOLINA, C. , & LOPEZ-MORENO, J. I. 2015. Contribution of precipitation and reference evapotranspiration to drought indices under different climates. *Journal of Hydrology,* 526, 42-54.

VICENTESERRANO, S. M., BEGUERÍA, S., LORENZOLACRUZ, J., CAMARERO, J. J., LÓPEZMORENO, J. I., AZORINMOLINA, C., REVUELTO, J., MORÁNTEJEDA, E. & SANCHEZLORENZO, A. 2012. Performance of Drought Indices for Ecological, Agricultural, and Hydrological Applications. *Earth Interactions,* 16, 1-27.

WAGLE, P., GOWDA, P. H., XIAO, X. & ANUP, K. C. 2016. Parameterizing ecosystem light use efficiency and water use efficiency to estimate maize gross primary production and evapotranspiration using MODIS EVI. *Agricultural & Forest Meteorology,* 222, 87-97.

WANG, J., WANG, K., ZHANG, M. & ZHANG, C. 2015a. Impacts of climate change and human activities on vegetation cover in hilly southern China. *Ecological Engineering,* 81, 451-461.

WANG, W., ZHU, Y., XU, R. & LIU, J. 2015b. Drought severity change in China during 1961–2012 indicated by SPI and SPEI. *Natural Hazards,* 75, 2437-2451.

WU, H., SVOBODA, M. D., HAYES, M. J., WILHITE, D. A. & WEN, F. 2007. Appropriate application of the standardized precipitation index in arid locations and dry seasons. *International Journal of Climatology,* 27, 65-79.

XIE, H., RINGLER, C., ZHU, T. & WAQAS, A. 2013. Droughts in Pakistan: a spatiotemporal variability analysis using the Standardized Precipitation Index. *Water international,* 38, 620-631.

XIN, J., ZHA, T., GONG, J., WANG, B., ZHANG, Y., WU, B., QIN, S. & PELTOLA, H. 2016. Carbon and water exchange over a temperate semi-arid shrubland during three years of contrasting precipitation and soil moisture patterns. *Agricultural & Forest Meteorology,* 228-229, 120-129.

XU, K., YANG, D., YANG, H., LI, Z., QIN, Y. & SHEN, Y. 2015. Spatio-temporal variation of drought in China during 1961–2012: A climatic perspective. *Journal of Hydrology,* 526, 253-264.

XUE, B. L., GUO, Q., OTTO, A., XIAO, J., TAO, S. & LE, L. 2015. Global patterns, trends, and drivers of water use efficiency from 2000. *Ecosphere,* 6**,** 174.

YANG, J., GONG, D., WANG, W., HU, M. & MAO, R. 2012. Extreme drought event of 2009/2010 over southwestern China. *Meteorology & Atmospheric Physics,* 115**,** 173-184.

YANG, Y., GUAN, H., BATELAAN, O., MCVICAR, T. R., LONG, D., PIAO, S., LIANG, W., LIU, B., JIN, Z. & SIMMONS, C. T. 2016a. Contrasting responses of water use efficiency to drought across global terrestrial ecosystems. *Sci Rep,* 6**,** 23284.

YANG, Y., GUAN, H., BATELAAN, O., MCVICAR, T. R., LONG, D., PIAO, S., LIANG, W., LIU, B., JIN, Z. & SIMMONS, C. T. 2016b. Contrasting responses of water use efficiency to drought across global terrestrial ecosystems. *Scientific reports,* 6**,** 1-8.

YU, G., CHEN, Z., PIAO, S., PENG, C., CIAIS, P., WANG, Q., LI, X. & ZHU, X. 2014. High carbon dioxide uptake by subtropical forest ecosystems in the East Asian monsoon region. *Proceedings of the National Academy of Sciences,* 111**,** 4910-4915.

YU, G., SONG, X., WANG, Q., LIU, Y., GUAN, D., YAN, J., SUN, X., ZHANG, L. & WEN, X. 2008. Water-use efficiency of forest ecosystems in eastern China and its relations to climatic variables. *New Phytol,* 177**,** 927-37.

ZHAI, JIANQING, BUDA, S. U., KRYSANOVA, VALENTINA, VETTER, TOBIAS, GAO, C. & JIANG, T. 2010. Spatial Variation and Trends in PDSI and SPI Indices and Their Relation to Streamflow in 10 Large Regions of China. *Journal of Climate,* 23**,** 649-663.

ZHANG, J., JIANG, L., FENG, Z. & LI, P. 2012. Detecting Effects of the Recent Drought on Vegetation in Southwestern China. *Journal of Resources & Ecology,* 3**,** 43-49.

ZHANG, Y., WANG, Y., ZHANG, M. & MA, K. 2014. Climate change threats to protected plants of China: an evaluation based on species distribution modeling. *Chinese Science Bulletin,* 59**,** 4652-4659.

ZHANG, Y., XIAOMING, F., XIAOFENG, W. & BOJIE, F. 2018. Characterizing drought in terms of changes in the precipitation–runoff relationship: a case study of the Loess Plateau, China. *Hydrology & Earth System Sciences,* 22**,** 1749-1766.

ZHAO, M. & RUNNING, S. W. 2010. Drought-induced reduction in global terrestrial net primary production from 2000 through 2009. *science,* 329**,** 940-943.

ZHITAO, W., JIANJUN, W., BIN, H., JINGHUI, L., QIANFENG, W., HONG, Z. & YONG, L. 2014. Drought offset ecological restoration program-induced increase in vegetation activity in the Beijing-Tianjin Sand Source Region, China. *Environmental Science & Technology,* 48**,** 12108-17.

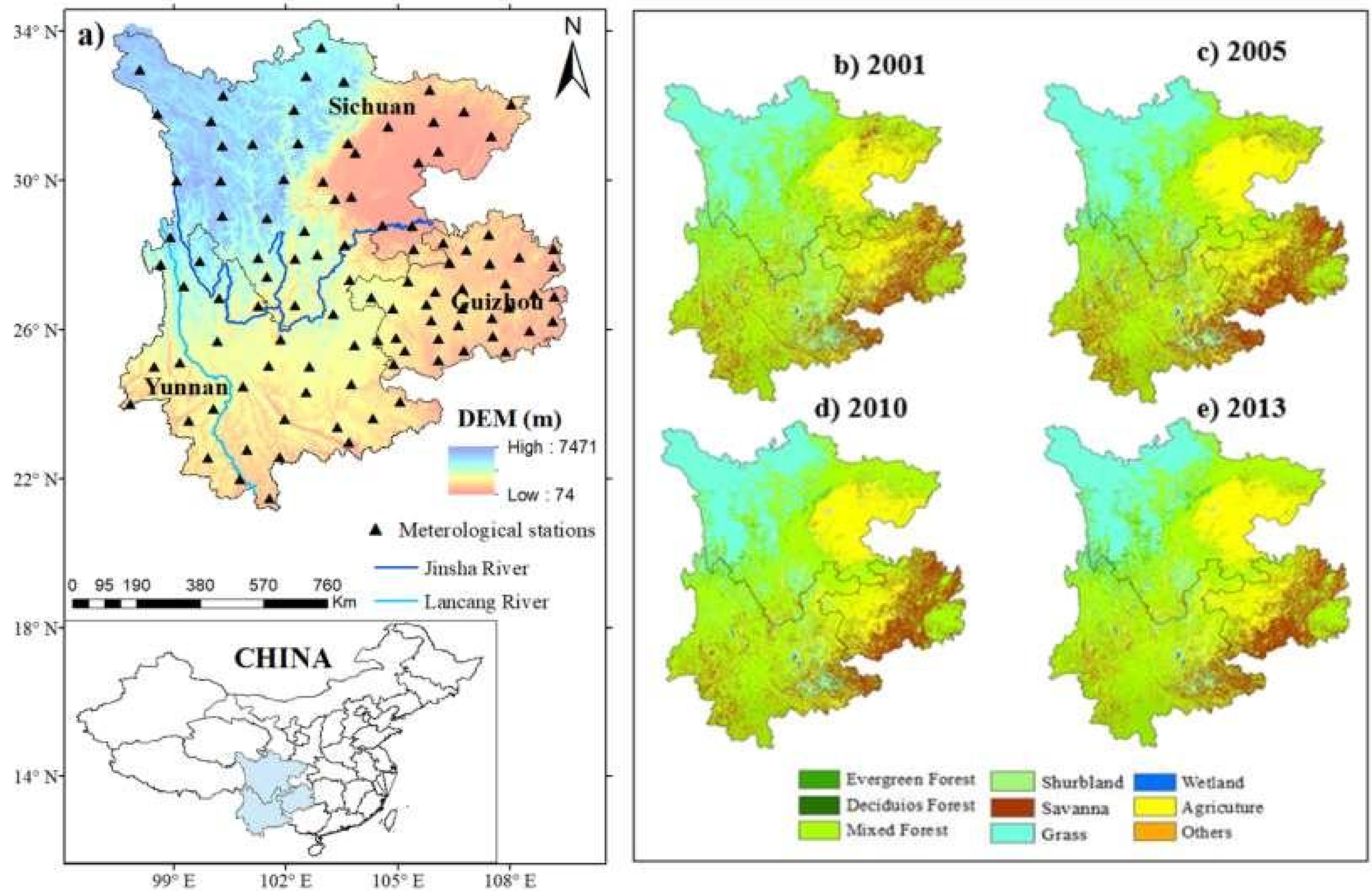

Figure 1: The location of the study area (a) and the spatial distribution of the ecosystem evolution from 2001 to 2013 (b-e).

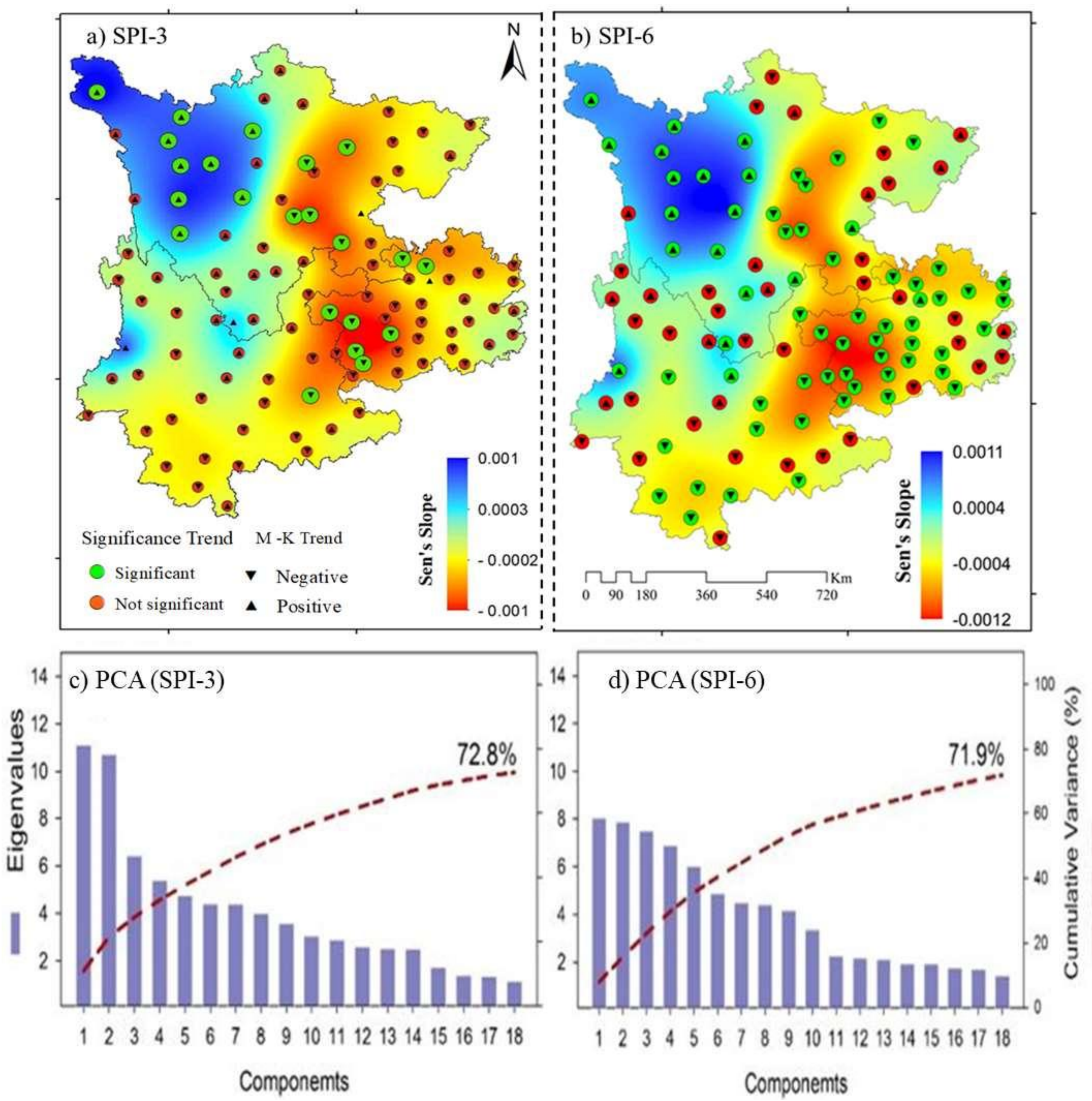

Figure 2: Spatial distribution of drought index (SPI-3 and SPI-6) and Scree plot of the cumulative variance explained by the components of the PCA for SPI-3 and SPI-6.

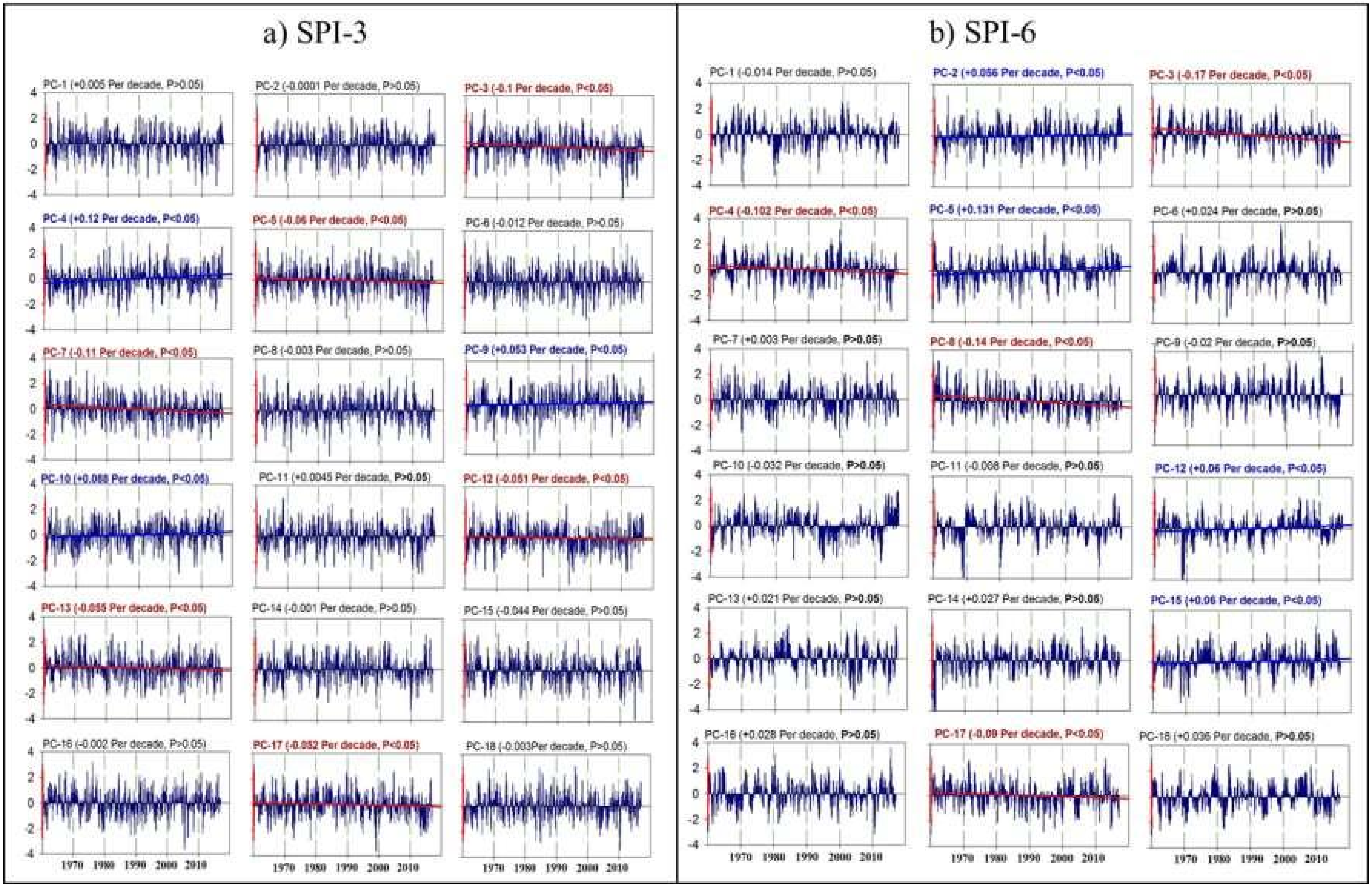

Figure 3: Temporal evolution and trends of the 3 and 6 monthly SPIs from the PCs' corresponding scores representing drought patterns in southwest China.

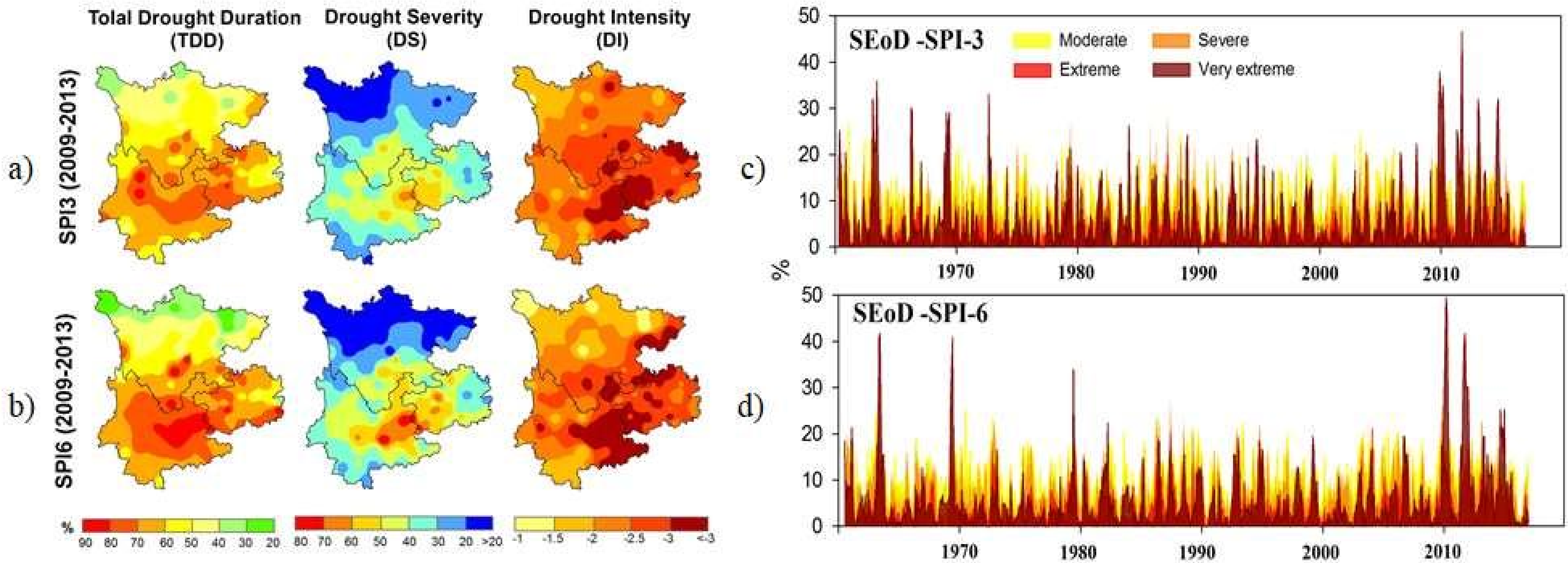

Figure 4: Spatial distribution of (TDD, %), drought severity (DS) and drought intensity (DI) during drought events (a, b) and the temporal evolution of spatial extent of drought (SEoD %, i.e., the percentage area affected by drought (c, d).

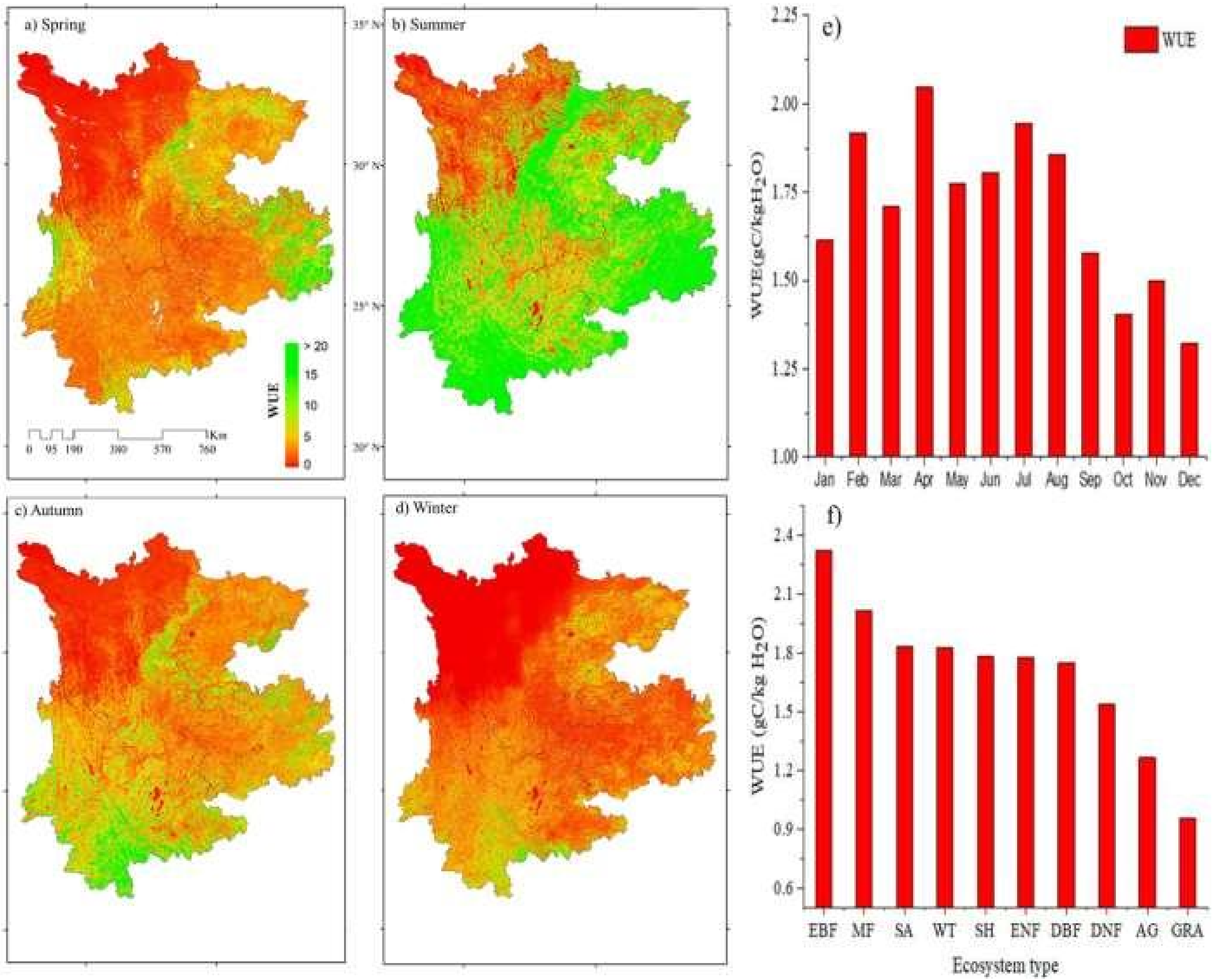

Figure. 5: Spatial distribution of WUE for the seasons (a-d), monthly changes in WUE (e) and WUE for the different ecosystem types (f) in southwest China during 2001-2016.

Note: (ENF: evergreen needle-leaf forests, EBF: evergreen broadleaf forests, DNF: deciduous needle-leaf forests, DBF: deciduous broadleaf forests, MF: mixed forests, SH: shrublands, SA: savannas, AG: agriculture, GRA: grass and WT: wetland

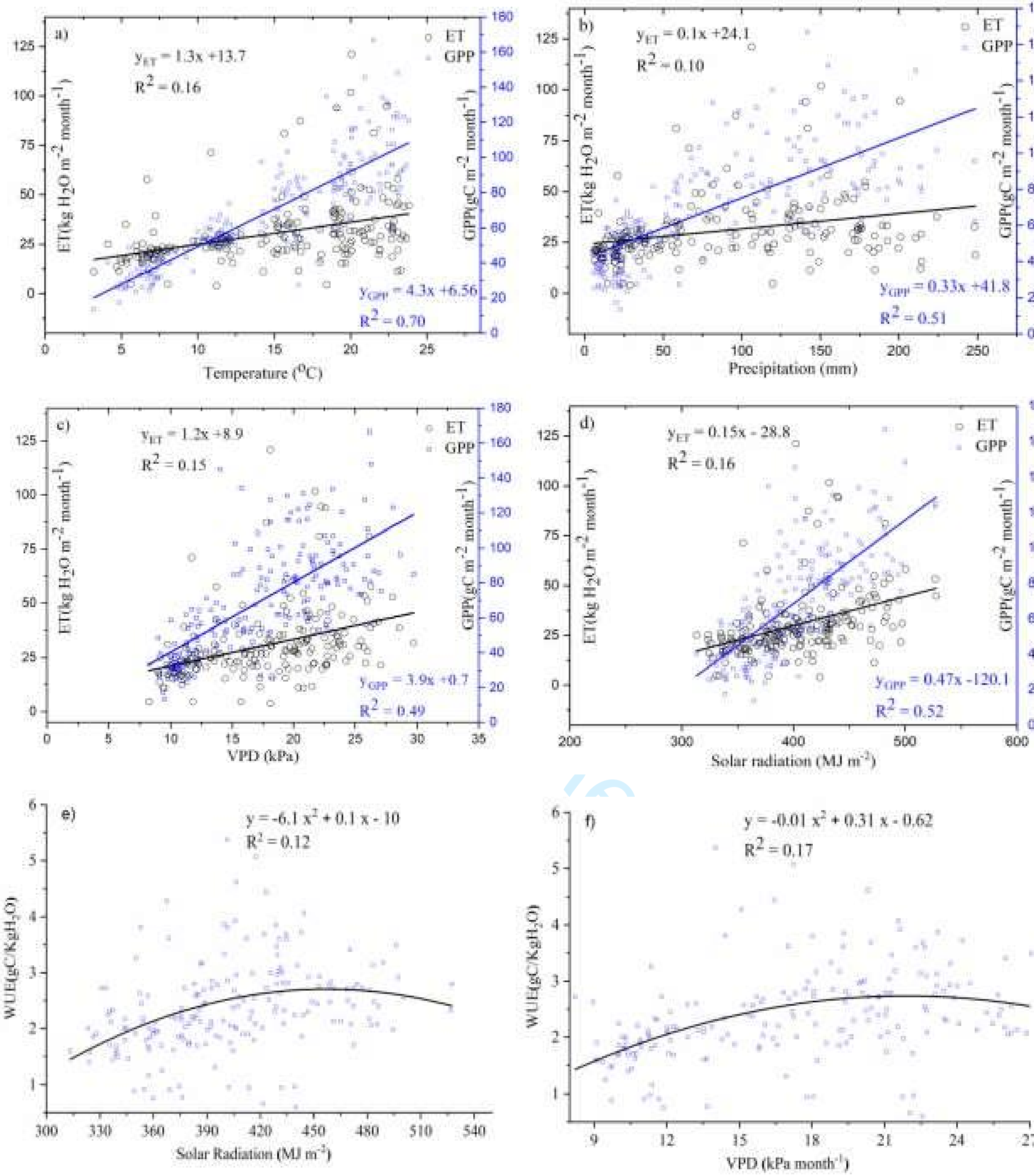

Figure 6: The monthly relationship of GPP and ET with the monthly temperature (a), precipitation (b), vapor pressure deficit (VPD) (c) and solar radiation (d)(a-d), relationship of monthly WUE with monthly solar radiation (e) and VPD (f) for the different ecosystems during 2001-2016.

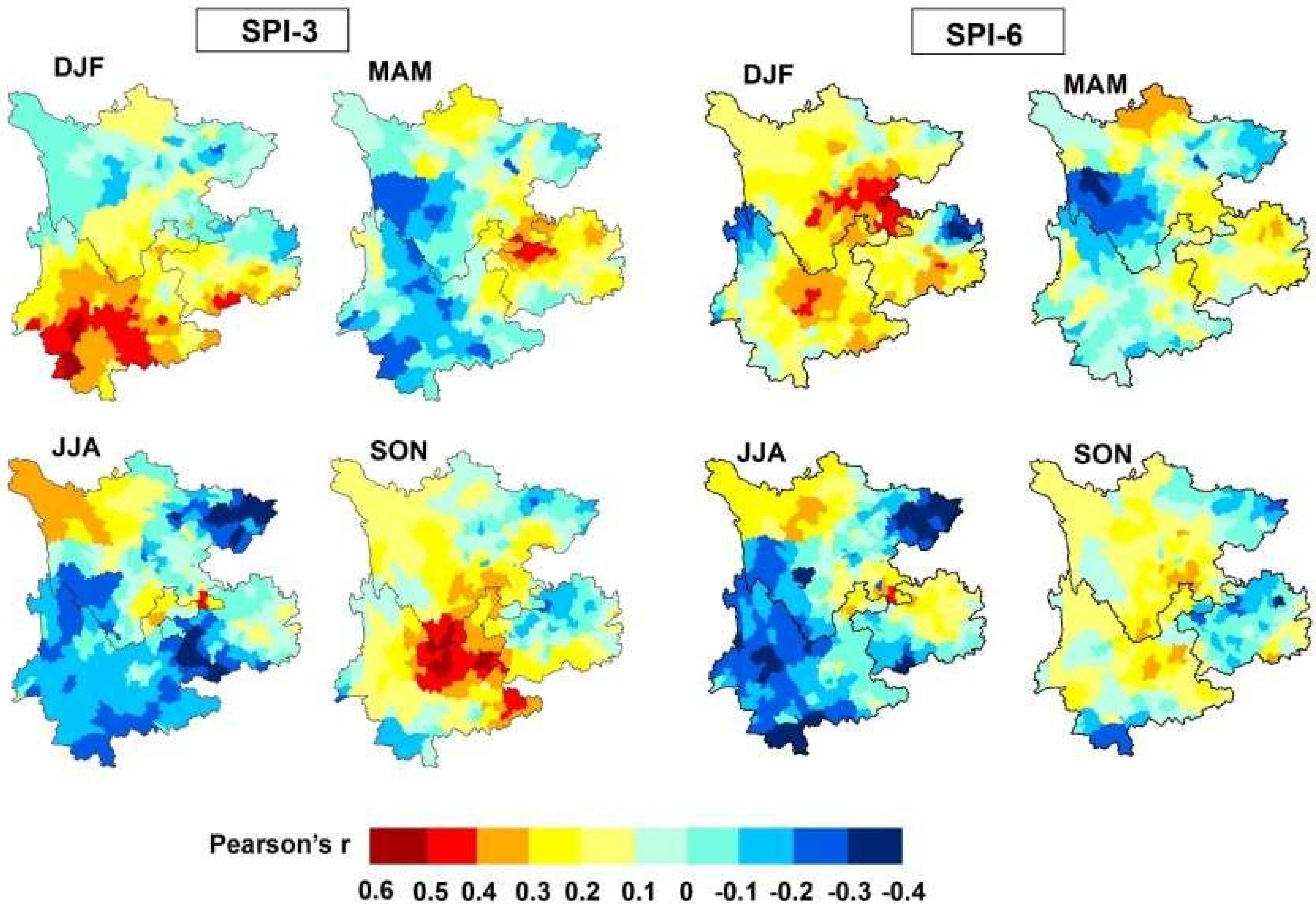

Figure 7: The spatial monthly distribution of Pearson correlation coefficient between WUE and the SPIs (winter - DJF: December, January and February; spring - MAM: March, April and May; summer - JJA: June, July, August; and autumn - SON: September, October and November.

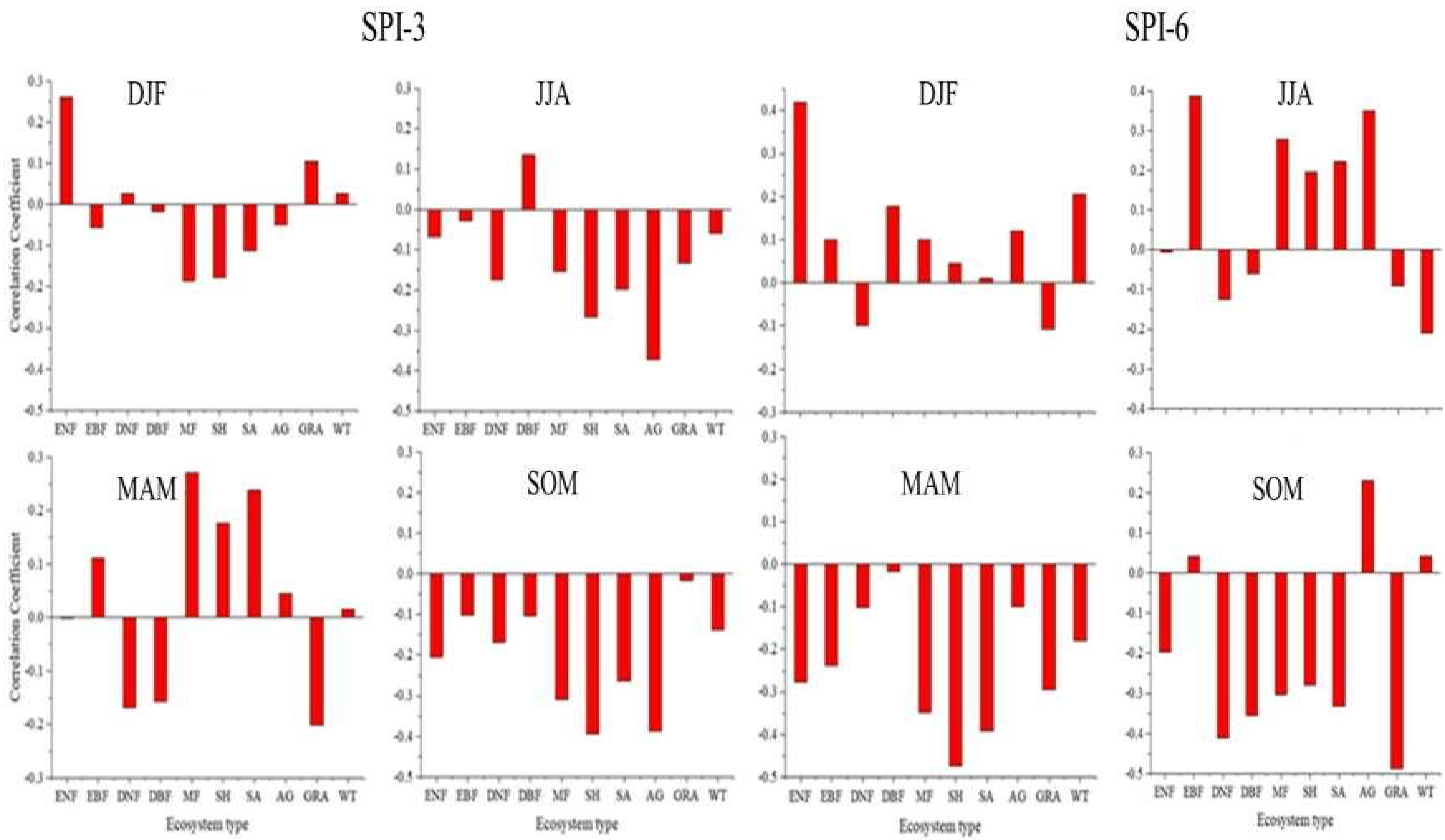

Figure 8: The regional monthly correlation coefficients between WUE and the SPIs for the different ecosystem types.

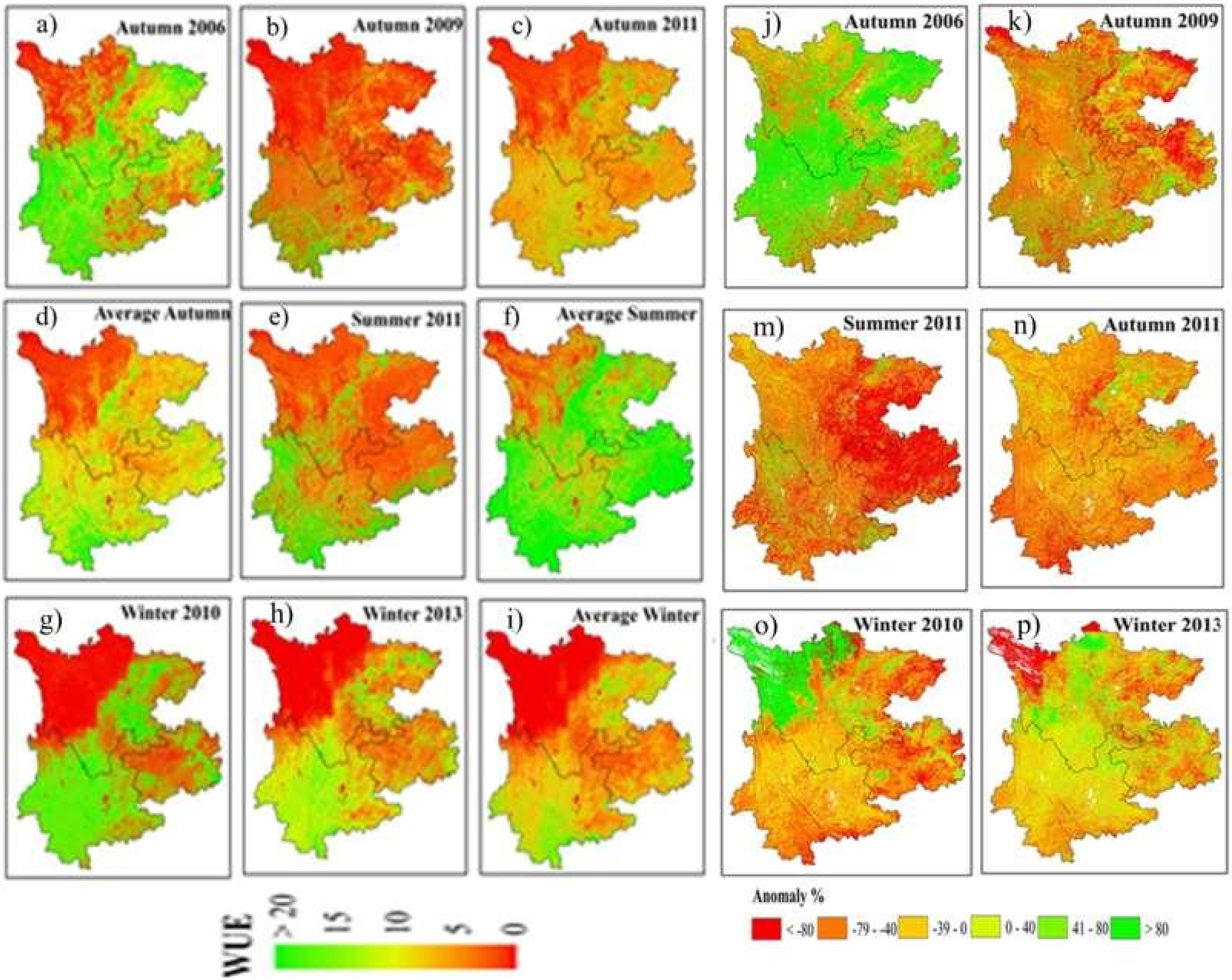

Figure 9: Spatial distribution of WUE for the seasons (a to i) and the magnitude and spatial patterns of the annual WUE anomalies (j to p).

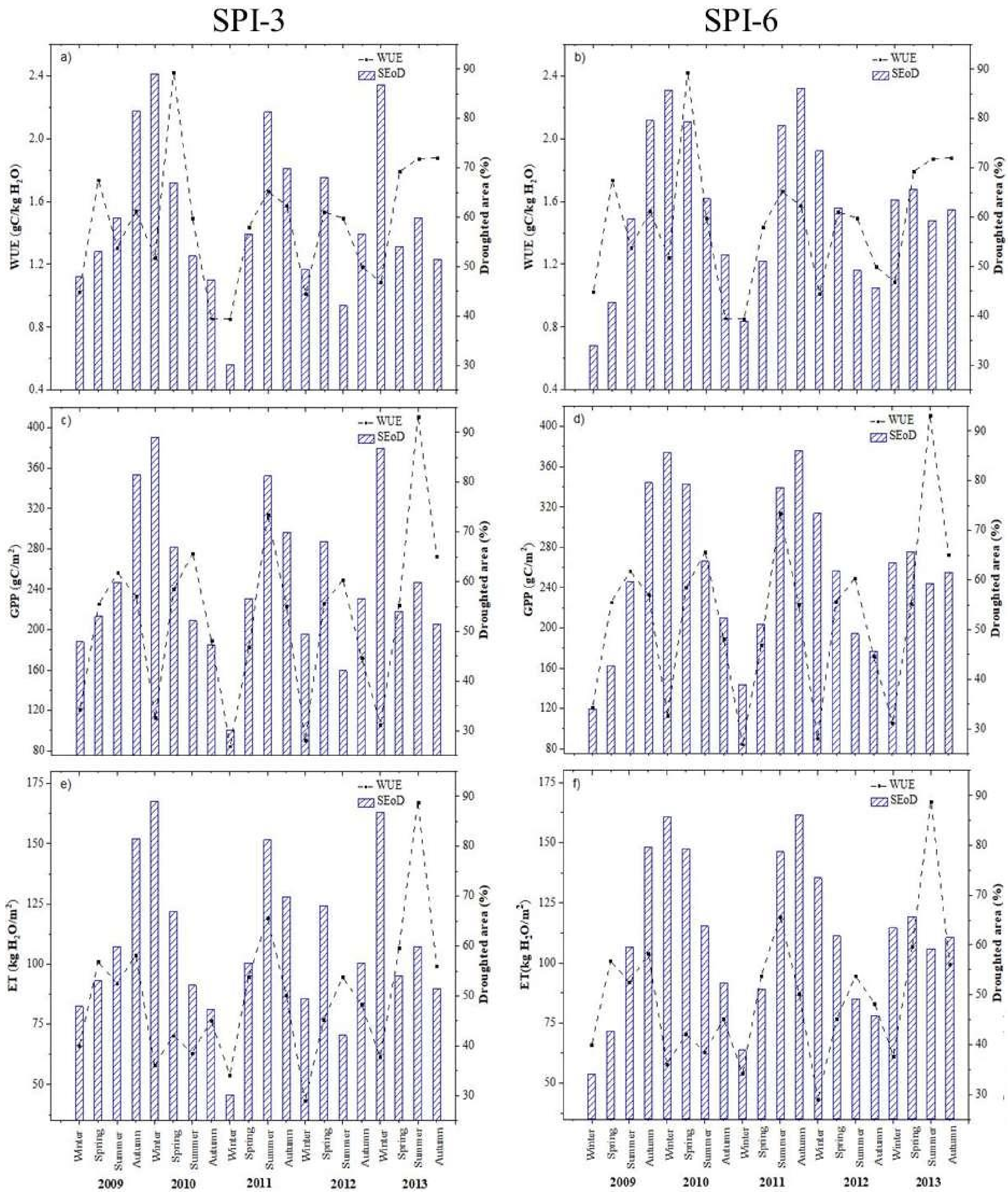

Figure 10: Seasonal variation of WUE, GPP and ET with percentage drought area (SEoD) during the drought events.

Figure 1: The location of the study area (a) and the spatial distribution of the ecosystem evolution from 2001 to 2013 (b-e).

Figure 2: Spatial distribution of drought index (SPI-3 and SPI-6) and Scree plot of the cumulative variance explained by the components of the PCA for SPI-3 and SPI-6.

Figure 3: Temporal evolution and trends of the 3 and 6 monthly SPIs from the PCs' corresponding scores representing drought patterns in southwest China.

Figure 4: Spatial distribution of (TDD, %), drought severity (DS) and drought intensity (DI) during drought events (a, b) and the temporal evolution of spatial extent of drought (SEoD %, i.e., the percentage area affected by drought (c, d).

Figure. 5: Spatial distribution of WUE for the seasons (a-d), monthly changes in WUE (e) and WUE for the different ecosystem types (f) in southwest China during 2001-2016.

Note: (ENF: evergreen needle-leaf forests, EBF: evergreen broadleaf forests, DNF: deciduous needle-leaf forests, DBF: deciduous broadleaf forests, MF: mixed forests, SH: shrublands, SA: savannas, AG: agriculture, GRA: grass and WT: wetland

Figure 6: The monthly relationship of GPP and ET with the monthly temperature (a), precipitation (b), vapor pressure deficit (VPD) (c) and solar radiation (d)(a-d), relationship of monthly WUE with monthly solar radiation (e) and VPD (f) for the different ecosystems during 2001-2016.

Figure 7: The spatial monthly distribution of Pearson correlation coefficient between WUE and the SPIs (winter - DJF: December, January and February; spring - MAM: March, April and May; summer - JJA: June, July, August; and autumn - SON: September, October and November.

Figure 8: The regional monthly correlation coefficients between WUE and the SPIs for the different ecosystem types.

Figure 9: Spatial distribution of WUE for the seasons (a to i) and the magnitude and spatial patterns of the annual WUE anomalies (j to p).

Figure 10: Seasonal variation of WUE, GPP and ET with percentage drought area (SEoD) during the drought events.

Table 1. The ecosystem area extent in southwest China between 2001and 2013 (km^2)

	2001	2005	2010	2013
Water bodies	1,360.71	1,129.09	995.79	1,017.04
Evergreen forest (EF)	48,227	53,811.72	55,162.77	75,024.04
Deciduous forest (DF)	5,271.74	1,481.55	1,276.56	1,554.32
Mixed forest (MF)	351,181.55	354,690.32	413,582.31	406,291.94
Shrub	29,817.67	4,661.04	3,061.43	2,957.53
Savanna	158,759.48	178,969.57	140,264.70	129,954.12
Grass	230,738.84	235,579.34	215,846.00	208,226.35
Wetland	2,703.81	3,138.70	4,302.57	1,185.33
Agriculture	209,584.48	204,663.70	203,642.58	212,186.75
Others	6,878.87	6,399.12	6,389.46	6,126.72

Table 2. Area transition matrix for the ecosystem types in southwest China between 2001 and 2013 (km^2)

	EF	DF	MF	Shrub	Savanna	Grass	Wetland	Agriculture	Total 2001
EF	32,735.4	23.3	11,662.6	9.2	1,157	244.5	65.7	2,312.5	48,210.4
DF	129.3	224.1	3,547	7.5	284.6	369.6	10.5	696.6	5,269.3
MF	24,669	587.7	264,667.5	495.9	26,719.4	10,848.8	246.9	22,912.7	351,147.9
Shrub	511.5	27.9	10,456.7	637.3	5,078.4	4,815.9	76.4	8,168.2	29,772.3
Savanna	8,698.8	133.5	56,624.4	440.3	63,400.9	3,602.2	186.1	25,651.1	158,737.3
Grass	3,343.3	287.4	18,773.2	761.8	7,735.2	179,164.2	81.4	20,323.2	230,469.8
Wetland	76.6	7.5	1395.5	13.7	428.7	12	80.9	679	2,694
Agriculture	4,673.5	260	39007.6	587.7	25130.5	8382.9	366.2	131,145.5	209,553.9
Total 2013	74,837.6	1,551.6	406,134.4	2,953.5	129,934.8	207,440.1	1,114.1	211,888.7	

Note: Values are the areas of row ecosystems that transformed into column ecosystems from 2001 to 2013.

Table 3 The Agnew's scheme for drought categories classification (Agnew, 2000).

Drought group	SPI values
No drought	> 0
No drought	0 to -0.5
Moderate drought	-0.5 to -0.84
Severe drought	-0.84 to -1.28
Extreme drought	-1.28 to -1.65
Very extreme drought	>-1.65

Table 4. The percentage areas having positive or negative correlation between water use efficiency (WUE) and the SPIs.

	SPI -3				SPI-6			
	Positive		Negative		Positive		Negative	
Season	Significant	Non-Significant	Significant	Non-Significant	Significant	Non-Significant	Significant	Non-Significant
Spring	8.03	50.14	0.55	41.27	4.71	61.50	0.83	32.96
Summer	2.22	31.30	8.59	57.89	4.16	34.63	11.08	50.14
Autumn	24.38	57.06	0.28	18.28	9.70	63.71	0.55	26.04
Winter	26.04	52.08	0.00	21.88	35.46	56.23	1.11	7.20

Table 5. Percentage of area (grid cells, %) with ΔWUE > 0 and ΔWUE < 0 in the drought seasons for the different ecosystem types in southwest China.

Ecosystem type	2006 Autumn		2009 Autumn		2010 Winter		2011 Summer		2011 Autumn		2013 Winter	
	Δ > 0	Δ < 0	> 0	Δ < 0	> 0	Δ < 0	> 0	Δ < 0	> 0	Δ < 0	> 0	Δ < 0
Forest	83.8	16.2	28.5	71.5	35	65	47.4	52.6	47.4	52.6	14.6	85.4
Shrub	100	0	26.2	73.8	20	80	41.6	58.4	41.6	58.4	2.1	97.9
Savanna	85	15	20.5	79.5	21.8	78.2	54.0	46.0	54	46	12.2	87.8
Agriculture	92.2	7.8	30.4	69.6	34.8	65.2	64.0	36.0	64	36	18.6	81.4
Grass	59.8	40.2	36.4	63.6	100	0	38.1	61.9	38.1	61.9	12.6	87.4

Table 6. Correlation coefficient between monthly water use efficiency (WUE) and the controlling climate factors for the ecosystem functional types.

	Ecosystem types	P	T	SR	VPD
WUE	ENF	0.87**	0.83**	0.74**	0.81**
	EBF	-0.72**	-0.83**	-0.68**	-0.65**
	DNF	0.70**	0.76**	0.82**	0.88**
	DBF	0.82**	0.83**	0.78**	0.87**
	MF	0.04	-0.04	0.03	0.18
	SH	0.34	0.39*	0.47*	0.59**
	SA	-0.22	-0.25	-0.19	-0.02
	AG	0.25	0.30	0.35*	0.55**
	GRA	0.85**	0.82**	0.69**	0.72**
	WT	0.38*	0.38*	0.46*	0.61**

Note: ** Correlation is significant at the 1% significance level and * Correlation is significant at the 5% significance level.

ENF: evergreen needleleaf forest; EBF: evergreen board forest; DNF: deciduous needleleaf forest; DBF: deciduous board forest; MF: mixed forest; SH: shrubland; SA: savanna; AG: agriculture; GRA: grass; WT: wetland; P: precipitation; T: temperature; SR: solar radiation; and VPD: vapor pressure deficit.